Simultaneous reconstruction of flow and temperature cross-sections in gases using acoustic tomography

Tat Hean Gan, David A. Hutchins,[a] and Peter W. Carpenter
School of Engineering, University of Warwick, Coventry CV4 7AL, United Kingdom

William M. D. Wright
Department of Electrical and Electronic Engineering, University College Cork, Ireland

(Received 15 January 2003; revised 2 May 2003; accepted 14 May 2003)

This paper describes the use of air-coupled ultrasonic tomography for the simultaneous measurement of flow and temperature variations in gases. Air-coupled ultrasonic transducers were used to collect through-transmission data from a heated gas jet. A transducer pair was scanned in two-dimensional sections at an angle to the jet, and travel time and amplitude data recorded along various paths in counter-propagating directions. Parallel-beam tomographic reconstruction techniques allowed images to be formed of variations in either temperature or flow velocity. Results have been obtained using heated jets, where it has been shown that it is possible to separate the two variables successfully. © *2003 Acoustical Society of America.* [DOI: 10.1121/1.1592523]

PACS numbers: 43.35.Ae, 43.38.Bs [DEC]

I. INTRODUCTION

Ultrasound has been used in many configurations to measure fluid flow, in both gas and liquid phases. The resulting instruments can be used in a wide range of applications in gases, such as industrial and domestic gas flow metering,[1] monitoring of gas flares on off-shore platforms,[2] and high-pressure gas flow measurement in gas distribution systems.[3] There are many measurements in liquids and in medical diagnosis that can also be performed. In liquids, ultrasonic flow meters have been used to measure very low liquid flow rates in the treatment of toxic liquids in semiconductor industries.[4] In medicine, ultrasound is now an established technique, such application being the measurement of blood flow in the nail bed of a human finger.[5]

The physical implementation of the technique usually relies on two main types of measurement—cross-propagation techniques[6] and Doppler measurements.[7] The cross-propagation technique is based on the transmission of ultrasound at a certain angle, and the change in time-of-flight of the transmitted ultrasound is related to the velocity of the flow. The Doppler technique is based on reflected or scattered ultrasonic signals from particles in the flow, which cause a shift in the received frequency content. While these two are the most common approaches to flow measurement using ultrasound, there are other methods such as cross-correlation,[8] vortex shedding[9] and open-channel measurements.[10]

Although such ultrasonic techniques have been available for some years, further improvements to achieve modern demands such as temperature compensation and measurement accuracy are limited.[11] For instance, work by Willatzen[12] has shown that the presence of temperature gradients can cause errors in flow estimation, because of changes in the local sound velocity.

In the present work, we were interested in using the ultrasonic tomographic technique to measure complex flows, where both flow and temperature gradients are present. Previous authors reported that acoustic tomography could be used to estimate fluid flow, remembering that flow is a vector quantity. For instance, fluid flow estimation was demonstrated both theoretically and experimentally,[13,14] using travel time measurements, and this was later extended to stratified fluid flow.[15] Diffraction tomography was also investigate for ultrasonic measurement of fluid flow.[16]

In the present case, we were particularly interested in the case of gas flow in turbulent jets, in the presence of temperature variations. This follows on from previous work,[17] where it was shown that either temperature or flow cross-sections could be measured in isolation using tomography. Here we present some experimental results, where it is shown that it is possible to reconstruct flow velocity and temperature variations simultaneously. This is illustrated for the particular case of a gas jet. Also included in this paper is a comparison between the ultrasonic technique and other scanned measurements systems, e.g., a hot-wire anemometer for flow and a thermocouple for temperature.

Tomographic reconstruction is a well-developed imaging technique that can be used to determine the cross-sectional values of a spatial by varying parameter from the transmission of acoustic signals through an object. This may be accomplished by transmitting an ultrasonic wave across the area of interest along a set of predetermined ray paths. There are many approaches to tomographic reconstruction. The first of these are iterative or series expansion methods, of which there are various approaches and methods of implementation.[18–22] This method is very flexible, in that it can correct for anisotropy and irregular geometries, although the result tends to be computationally intensive. Transform methods[23,24] are more efficient, but are less versatile and

[a]Author to whom correspondence should be addressed. Electronic mail: dah@eng.warwick.ac.uk

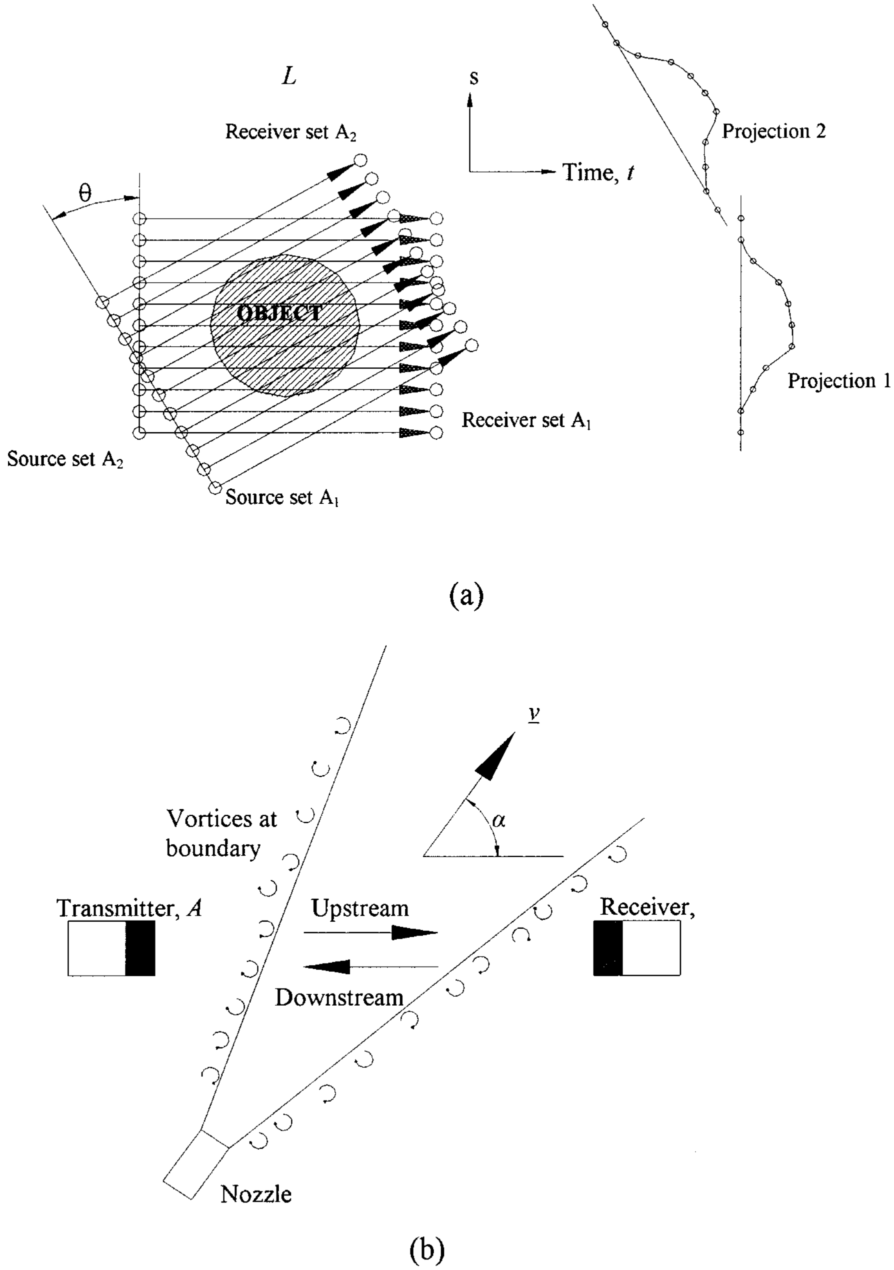

FIG. 1. (a) Schematic diagram of the parallel beam sampling geometry, defining the angle θ of each linear projection in the scan plane. (b) Configuration of the flow direction and the position of the transducers and hence scan plane at an angle α to the axis of a gas jet.

hence are not as popular. Probably the most widely used technique is filtered back-projection. This has been described in detail elsewhere.[25] It has the advantage in the present application that it is suitable for cylindrical scanning geometries of the type used here,[26] and is also fast and convenient to implement on a PC.

The present paper extends previous work, in that it shows that ultrasound can be used to reconstruct cross-sections in either flow or temperature, for fluid flow where both are varying spatially. In particular, it will be demonstrated that this can be done in gases, for a heated gas jet, using a combination of well-designed transducers and instrumentation, and appropriate measurement of the correct parameters for tomographic reconstruction. It also compares these results to those from point-to-point scanning of miniature flow and temperature sensors, demonstrating that the technique has some validity.

II. THEORETICAL BASIS OF THE TECHNIQUE

The technique uses a pair of ultrasonic capacitance transducers, which are highly efficient devices for generating ultrasonic signals in air. Their design is based on a micromachined silicon rigid backplate and a flexible Mylar membrane. The device construction is fully detailed elsewhere,[27] but the devices work well over the approximate frequency range of 100 kHz to 1 MHz. In the present measurements, a pair of such transducers, one acting as a source and the other as a receiver, was scanned in unison around the plane of interest using a simple "translate-rotate" sheme. This is shown schematically in Fig. 1, where the two transducers were fixed at points A and B, at a distance L apart. The transducer pair was scanned linearly across the region of interest, with a sampling interval of Δs [Fig. 1(a)]. When a projection was completed, the transducer pair was then rotated through an angle θ in the plane of measurement, as again illustrated in Fig. 1(a). The process of translation and rotation was then repeated up to 360°, so that signals could be propagated along the same paths in opposite directions, as required for the reconstruction process. Due to the discrete sampling of projections, the spatial sampling interval was limited by the Nyquist sampling theorem, and this is given by $B=1/2\Delta s$, where B is the spatial bandwidth and Δs is the linear spacing of each ray.

For each ray-path, the transit time of the transmitted signal t_{AB} was recorded, and used to estimate the change in local sound velocity across the area of interest [as shown in Fig. 1(b) for a gas jet, with the ray-path at some angle α to the jet axis]. However, as stated above, t_{AB} will depend on two main factors. The transit time will increase and decrease with the speed depending on the flow direction. In addition, the local temperature (T) also affects the speed of sound (c) according to the following dependence, quoted from previously published work:[28]

$$c=331.31\sqrt{\frac{T}{273.16}}\ \mathrm{ms}^{-1}. \tag{1}$$

Hence, both temperature T and flow velocity $\underline{v}$ can cause a change in the apparent value of sound speed. The former is a scalar effect, whereas flow is a vector quantity, and it is this information that can be used to distinguish their contribution to t_{AB}.

Assume that, in still air at some temperature T, the local sound speed is c_o. In the absence of flow, the acoustic travel time, t, across a distance L is given by $t=L/c_o$. When flow is present and properties, such as temperature, vary across the flow region, the acoustic travel time is altered by the effect of both U_θ (the component of the flow velocity in direction AB), and by any changes δc in the acoustic speed due to changes in T, so that the acoustic travel time becomes

$$t_{AB}=\frac{L}{c_0+(1/L)\int_0^L(\delta c+U_\theta)dx'}, \tag{2}$$

where the integral takes account of variations in both U_θ and δc across the flow region. For low-speed flow it can be assumed that

$$|\delta c+U_\theta|\ll c_0, \tag{3}$$

so that, to a good approximation,

$$t_{AB}-\frac{L}{c_0}=-\frac{1}{c_0^2}\int_0^L(\delta c+U_\theta)dx'. \tag{4}$$

For the ray going from B to A, U_θ changes sign, so that when the two opposing acoustic travel times are added, the contribution from the flow speed of the gas cancels, leaving the total contribution S_θ from the temperature variations along the selected path between the transducers only:

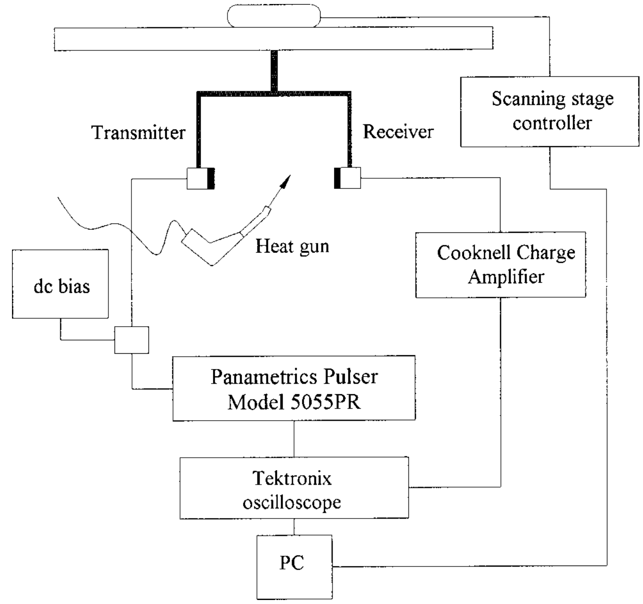

FIG. 2. A schematic diagram of the experimental arrangement for tomographic imaging.

$$S_\theta=t_{AB}+t_{BA}-\frac{2L}{c_0}=-\frac{2}{c_0^2}\int_0^L\delta c\,dx. \tag{5}$$

Similarly, subtracting the travel times gives

$$D_\theta=t_{AB}-t_{BA}=-\frac{2}{c_0^2}\int_0^L U_\theta dx', \tag{6}$$

and the integrated contribution (D_θ) is due only to gas flow. Hence, if ultrasonic signals are sent in counter-propagating directions along each ray path, addition of time of arrival would allow variations in δc [and hence temperature, via Eq. (1)] to be reconstructed, whereas subtraction leads to the measurement of variations in U_α (i.e., variations in the flow velocity) at the angle α. Flow and temperature can thus be measured independently in the same experiment.

Below, it is demonstrated that the use of well-designed transducers, operating at frequencies of up to 1 MHz, can be used in air to collect tomographic data from flowing gases at a range of temperatures. This information can then be used to reconstruct images of both temperature and flow variations independently. The technique is demonstrated using gas jets at both room temperature and at elevated temperatures.

III. APPARATUS AND EXPERIMENT

Figure 2 shows the apparatus used to perform ultrasonic measurements of flow and temperature in gas jets. One form of jet was created using a Steinel Model HL1605s heat gun, shown in the figure, with a 22-mm-diam nozzle. This provided an approximate volumetric flow rate of 250 $\mathrm{l\,min}^{-1}$ at temperatures of up to 50 °C at the plane of measurement. The ultrasonic capacitance transducers were separated by a distance of 142 mm, and were mounted horizontally as shown in the figure on a computer-controlled X-Y scanning

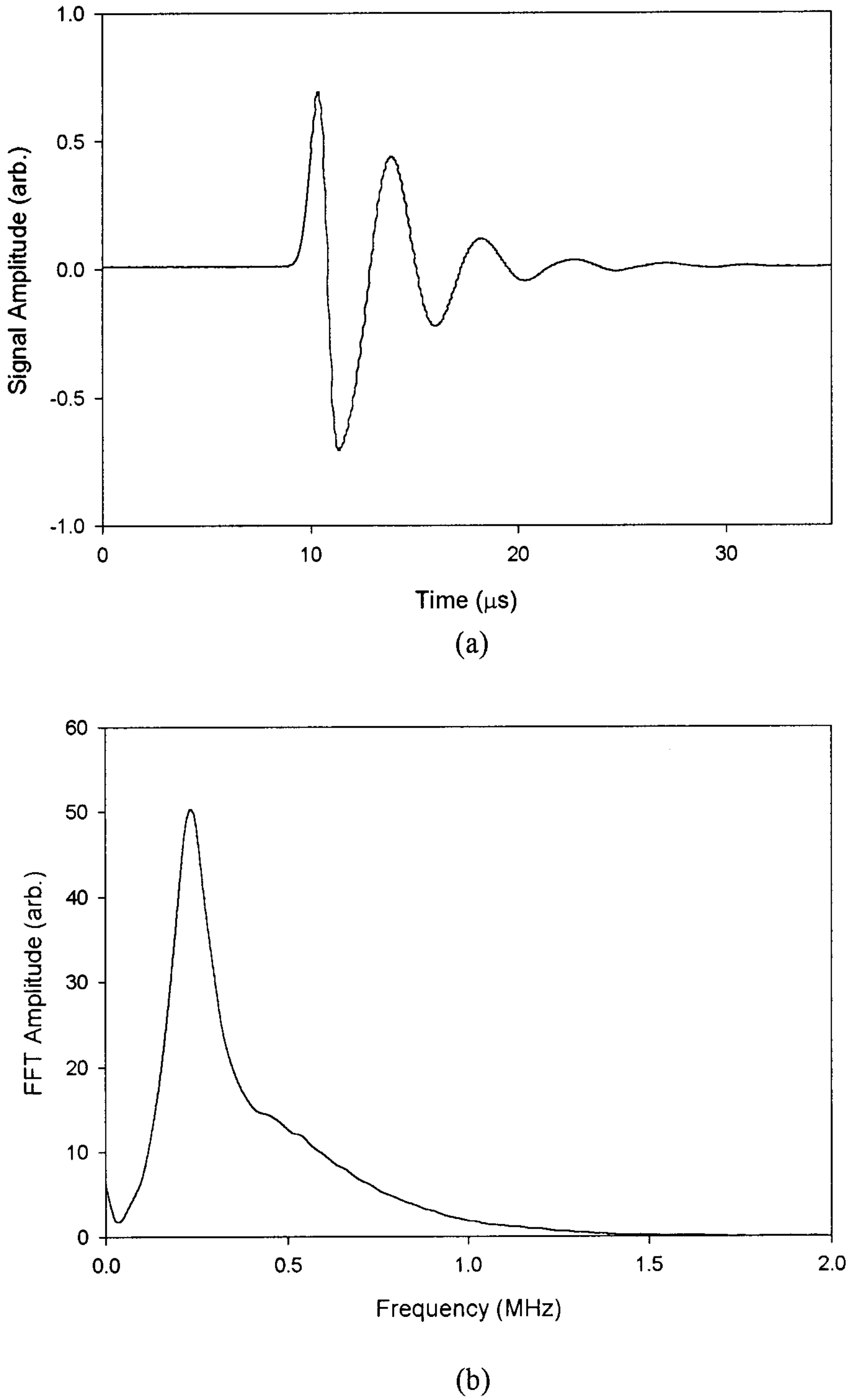

FIG. 3. A typical signal transmitted from source to receiver in the absence of gas flow, showing (a) a time waveform and (b) the corresponding spectrum.

stage. Each of the transducers could act as either a transmitter or receiver, so that signals could be transmitted in either direction through the selected region of flow. Time waveforms were recorded in each location on the digital oscilloscope, and transferred to the PC for automated software picking of arrival time t_{AB}.

The transducers, described more fully elsewhere,[26] were designed to have an excellent bandwidth and sensitivity for operation in air. A Panametrics 5055PR pulser provided voltage transients for excitation of the source, this being superimposed on a +100-V dc bias to attract the polymer film onto the backplate, to improve bandwidths. The receiver was connected to a Cooknell CA6/C charge amplifier, which again supplied the receiver with a 100-V dc bias. The results were then digitized using a Tektronix TDS540 oscilloscope before storing the arrival time for further data processing. Figure 3 shows a typical waveform transmitted from one device to the other in the absence of gas flow. The time response is well-damped, and the frequency response demonstrates that a reasonable bandwidth was available for the measurement. This improved the accuracy of time-of-flight measurements, which could then be fed into Eqs. (5) and (6).

Each full tomographic scan consisted of 61 linear projections ($\theta=3°$), each of which had 101 rays for which an

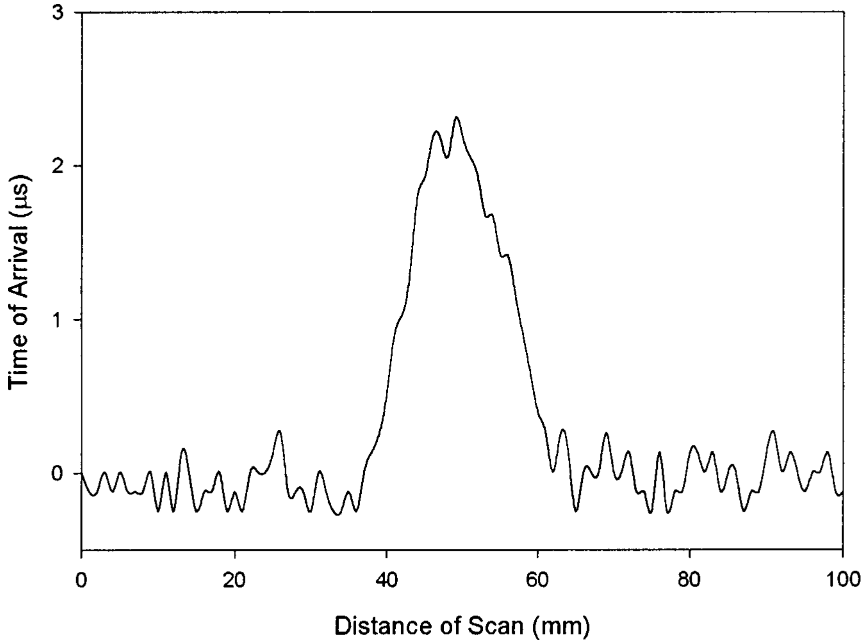

FIG. 4. Variation of time of flight (in μs) at a distance of 15 mm above a heat gun, measured using a through-transmission ultrasonic technique. The gas jet was heated and of approximately 28 mm diameter.

ultrasonic waveform was recorded at every 1-mm interval. Each projection involved scanning the transducers at right angles to their propagation axis using the linear stage. This was also attached to a rotational stage, so that projections could be taken at various angles in the plane of interest. Note that for all scans reported, a difference technique was employed to remove variations in room temperature and any unknown delays that might affect the ultrasonic time of flight. This was carried out by normalizing the data from each projection to the first waveforms taken in the ambient still air, outside the gas jet volume. Thus, systematic variations in room temperature or other factors were removed from the data prior to reconstruction. Data was collected in the form of time waveforms for each path. Note that at any one time there was only one signal to be recorded, using a single source–receiver pair. At no stage was there mixing of signals from multiple sources. In the case of counter-propagating signals along the same path, the source and receiver were interchanged in space during the 360° scan.

To provide independent measurements with which to compare the tomographic reconstructions from ultrasonic data, two point measurement devices were also scanned across the measurement plane. The first was a hot-wire anemometer (Model TA5 by Airflow Developments Ltd.), which measured flow velocity in a particular direction. The second was a K-type thermocouple, attached to a 9-V voltage supply unit, which measured the local temperature at that point. The same X-Y stage and control electronics was used for these scans, so that direct comparisons could be made.

Flow and temperature measurements, using both the ultrasonic tomography approach and the point detectors, were performed for various values of α, the angle between the gas jet axis and the plane containing the tomographic scan. Initial experiments were performed with the angle α between the gas jet axis and the tomographic scan plane [see Fig. 1(b)] at 90°, i.e., with the measurement plane perpendicular to the axis of flow (to enhance sensitivity to temperature

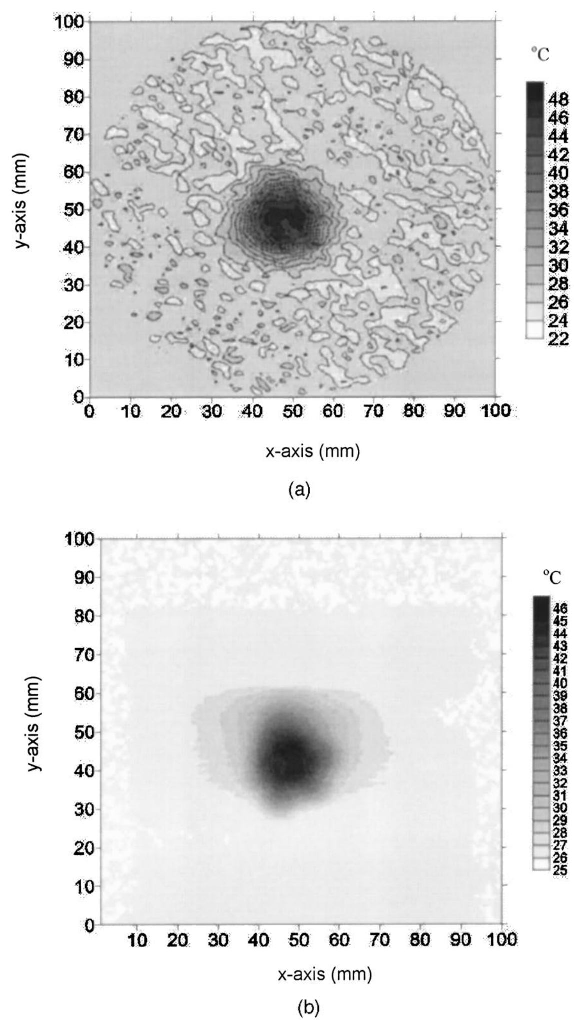

FIG. 5. Temperature measurement at 15 mm above the heated air jet from the heat gun, using (a) ultrasonic tomographic reconstruction and (b) a scanned thermocouple. $\alpha = 90°$ for this measurement so that the effects of temperature were maximized.

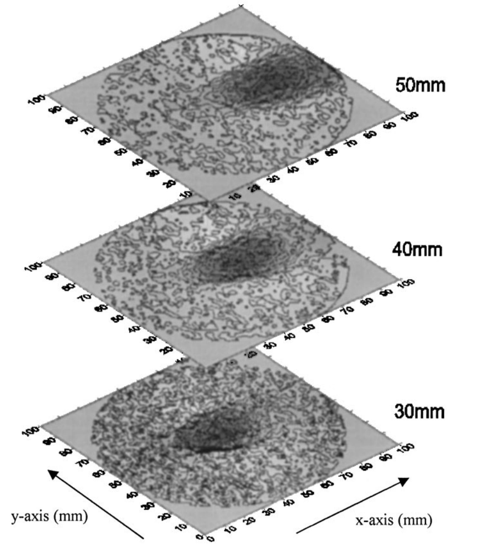

FIG. 6. Tomographic reconstruction of air flow velocity within the jet from the heat gun at different heights. The scan was performed at $\alpha = 45°$.

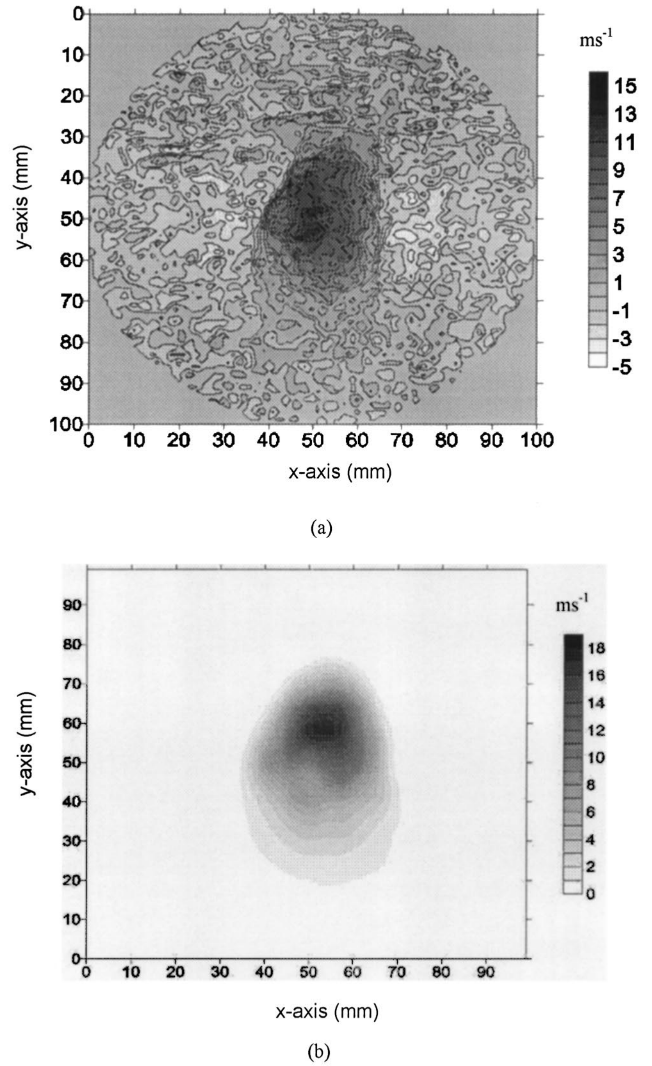

FIG. 7. Details of flow velocity cross-sections at a distance of 30 mm above the heat gun. Shown are the results of (a) tomographic reconstruction from ultrasonic data and (b) a scanned hot-wire anemometer.

effects with respect to flow). Other measurements were then performed at $\alpha = 45°$, at various vertical heights above the exit nozzle, so that both temperature and flow effects would contribute to the measurements. A final measurement was also made with the heat gun at $\alpha = 40°$, so that the effect of flow would be further enhanced.

IV. RESULTS AND DISCUSSION

A. Temperature measurements at $\alpha = 90°$

Experiments were performed initially to establish whether temperature variations could be reconstructed, using Eq. (5), without the effects of flow being a major factor. Data were thus collected with the gas jet vertical, and with the tomographic X-Y scan plane in the horizontal plane, i.e., with $\alpha = 90°$, where the effect of flow would be minimized. Note that the choice of $\alpha = 90°$ optimized the sensitivity of the measurement to temperature effects in relation to the effect of flow (which increases as α decreases). The scans were performed at a height of 15 mm above the heat gun. The results of ultrasonic measurements, leading to cross-sections of temperature via Eq. (1), were then compared to temperature cross-sections measured across the same plane using the thermocouple. The time of arrival of the ultrasonic signal was found to change by about 2.3 μs across the heated gas jet region of approximately 28 mm diameter, as shown in Fig. 4.

Figure 5(a) shows a tomographic reconstruction of the temperature profile 15 mm above the nozzle, obtained using ultrasonic data. This image can be compared to that obtained using the thermocouple [Fig. 5(b)]. The darker areas in both images represent the heated area and the size is well correlated. Both have a diameter of approximately 25 mm, with the temperature range being very similar. This demonstrates that the ultrasonic approach shows promise for completely noninvasive measurement of temperature variations in gases.

B. Simultaneous measurements of temperature and flow at $\alpha = 45°$

The direction of the heat gun was now set to $\alpha = 45°$ to the horizontal scanning plane. This made the measurement sensitive to components arising from both temperature and flow effects, the latter increasing in dominance as α increased in value. Equations (5) and (6) were used to obtain variations in δc [and hence temperature, via Eq. (1)] and U_θ across the same area of flow, using addition and subtraction of the counter-propagating ultrasonic signals along each ray path. The result was the simultaneous reconstruction of temperature and flow cross-sections.

The tomographic reconstruction of flow velocity images was performed using ultrasonic data at axial distances of 30, 40, and 50 mm from the exit nozzle, as shown in Fig. 6, and the maximum value of flow velocity at each the vertical height was found to be approximately 15.5, 12.5 and 11 ms^{-1}, respectively. As distance from the nozzle increased, the gas jet is seen to diverge, and the axial flow velocities reduce, as would be expected. At a distance of 30

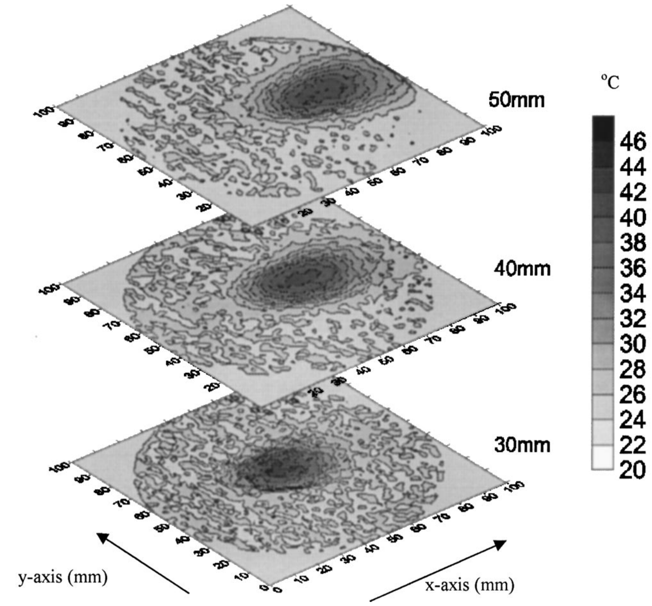

FIG. 8. Tomographic reconstruction of temperature variations, resulting from a scan at $\alpha = 45°$ of the heat gun at different heights.

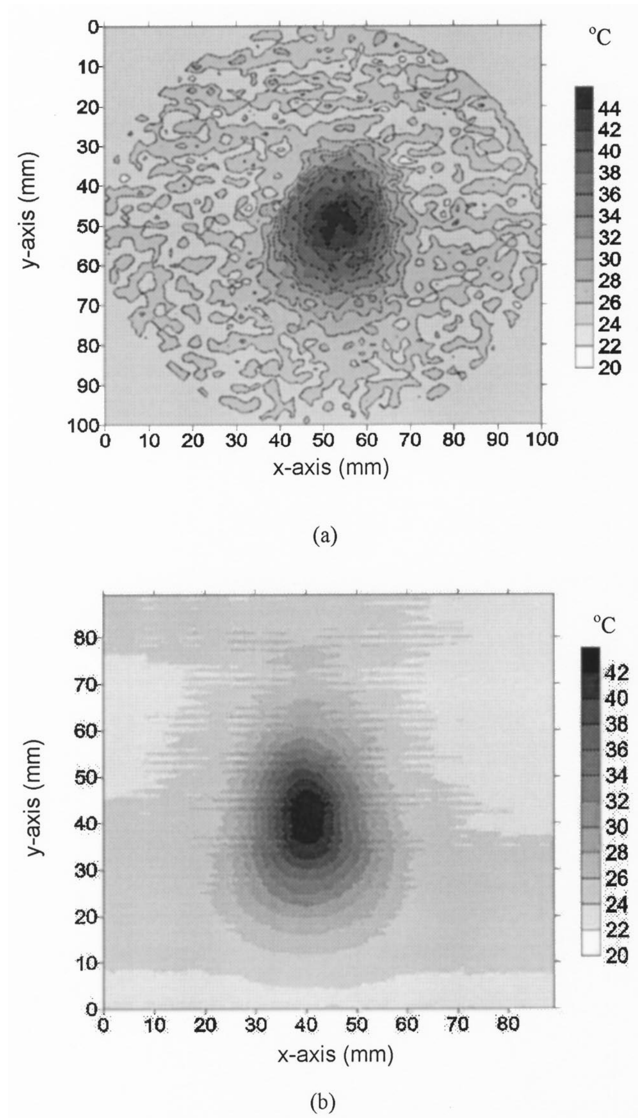

FIG. 9. Comparison of temperature cross-sections at a distance of 30 mm above the heat gun. (a) Temperature map derived from ultrasonic data and (b) measured via a scanned thermocouple.

mm, the hot wire anemometer was also scanned across the same area, to compare variations in axial flow velocity with those obtained from tomographic reconstruction. The maximum velocity detected by the point detector was found to be approximately $20\ \mathrm{ms}^{-1}$, and this agreed reasonably well with the value obtained from ultrasonic measurements, as shown in Fig. 7, where the two flow velocity cross-sections are compared.

Figure 8 shows the cross-sections in temperature that were reconstructed from ultrasonic data, at the three same heights above the heat gun nozzle as those shown earlier in Fig. 6. It will be evident from the figure that, as the axial distance from the exit nozzle increased, the average temperature reduced, as would be expected (these are displayed as lighter shades on the images). Note that, as before, the divergence of the hot air jet is evident as the increased diameter with axial distance. Note also that temperatures at 10 mm axial distances from the nozzle were predicted to approach 50 °C.

Figure 9(a) shows the reconstructed image at a height of 30 mm. This is compared to the measurements from the thermocouple, scanned as appoint detector over the same area, and presented in Fig. 9(b). The images show that the two results are similar to within a few degrees.

C. Measurements at $\alpha = 40°$

As a final experiment, the flow angle was reduced to 40°. This was performed so that the sound propagation is affected more by the flow and less by variations in temperature. The reconstructed image at the vertical height of 30 mm is as shown in Fig. 10(a). The hot-wire anemometer result is presented in Fig. 10(b). The flow imaging seems to be more successful as the velocity is now closer to the value imaged using the anemometer. It can thus be concluded that $\alpha = 40°$ can be used to optimize flow measurements for the same heated gas jet. Note that changing the angle would have little effect on the reconstruction of temperature profiles, as temperature is a scalar component of the equations. This has been observed in practice.

V. CONCLUSIONS

Ultrasonic tomographic imaging has been performed using a pair of broadband capacitance transducers to measure flow and temperature. A difference technique was employed to remove variations in room temperature and any unknown delays. This was carried out by normalizing the data from each projection to the first waveform in a particular linear scan, at some angle θ.

This experiment investigated the simultaneous reconstruction of temperature and flow velocity cross sections within a heated gas jet. The experiments were first conducted at $\alpha = 90°$ and it was shown that temperature measurement can be corrected by performing a 360° tomographic scan. When $\alpha = 45°$ it was shown that good results could be obtained if counter-propagating signals were used to separate

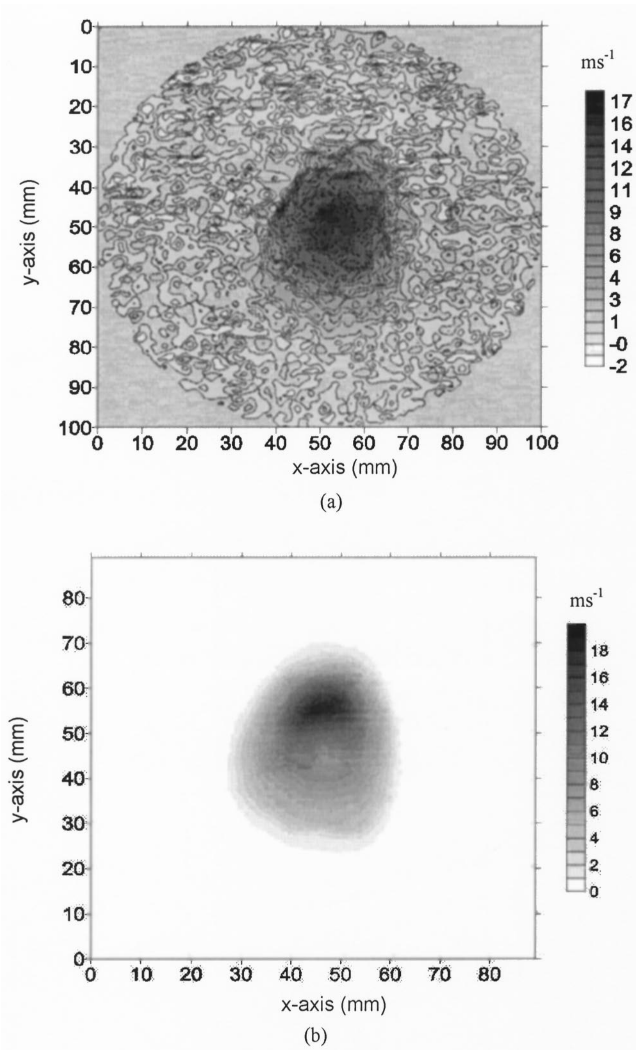

FIG. 10. Flow cross-sections taken at $\alpha=40°$ and at a height of 30 mm above the heat gun. (a) Flow velocity variations derived from acoustic data and (b) measured via a scanned hot wire anemometer.

the two components. It was found, however, that either flow or temperature measurement could be optimized by changing the angle α. Temperature would be best measured at $\alpha=90°$, so that flow effects were minimized. Conversely, temperature effects could be minimized by decreasing α to 45° or 40° and enhancing the effect of flow.

[1] G. Buonanno, ''On field characterization of static domestic gas flowmeters,'' Measurement **27**, 277–285 (2000).
[2] E. A. Hammer, ''Flare gas metering and high pressure gas metering using ultrasonic sensors,'' IEE Colloq. Ultra. Process Indus. **8**, 1–4 (1993).
[3] M. Dell'Isola, M. Cannizzo, and M. Diritti, ''Measurement of high-pressure natural gas flow using ultrasonic flowmeters,'' Measurement **20**, 75–89 (1997).
[4] M. Takamoto, H. Ishikawa, K. Shimizu, H. Monji, and G. Matsui, ''New measurement method for very low liquid flow rates using ultrasound,'' Flow Meas. Instrum. **12**, 267–273 (2001).
[5] D. E. Kruse, J. J. Mai, R. H. Silverman, M. F. Insana, D. J. Coleman, and K. W. Ferrara, ''Optimization of real-time high frequency ultrasound for blood flow imaging in the micro-circulation,'' Proc. SPIE **4325**, 284–292 (2001).
[6] R. C. Asher, ''Ultrasonic sensors for the process industry,'' Meas. Control **30**, 138–140 (1997).
[7] L. C. Lynnworth, *Ultrasonic Measurements for Process Control—Theory, Techniques, Applications* (Academic, London, 1989).
[8] V. Skwarek, H. Windorfer, and V. Hans, ''Measuring pulsating flow with ultrasound,'' Measurement **29**, 225–236 (2001).
[9] V. Hans, G. Poppen, E. von Lavante, and S. Perpeet, ''Vortex shedding flowmeters and ultrasound detection: signal processing and influence of bluff body geometry,'' Flow Meas. Instrum. **9**, 79–82 (1998).
[10] B. L. Thurley, ''The fundamentals of open channel flow measurement,'' in *Proc. Symp. Appl. of Flow Measuring Tech. (Flow-Con 77)* (1977), pp. 171–186.
[11] H. Köchnert, A. Melling, and M. Baumgärtner, ''Optical flow field investigations for design improvements of an ultrasonic gas meter,'' Flow Meas. Instrum. **7**, 133–140 (1996).
[12] M. Willatzen, ''Temperature gradients and flow-meter performance,'' Ultrasonics **39**, 383–389 (2001).
[13] S. J. Norton, ''Tomographic reconstruction of 2-D vector fields: application to flow imaging,'' Geophys. Res. **97**, 161–168 (1988).
[14] H. Braun and A. Hauck, ''Tomographic reconstruction of vector fields,'' IEEE Trans. Signal Process. **39**, 464–471 (1991).
[15] K. B. Winters and D. Rouseff, ''Tomographic reconstruction of stratified fluid flow,'' IEEE Trans. Ultrason. Ferroelectr. Freq. Control **40**, 26–33 (1993).
[16] M. N. Rychagov and H. Ermert, ''Reconstruction of fluid motion in acoustic diffraction tomography,'' J. Acoust. Soc. Am. **99**, 3029–3035 (1996).
[17] W. M. D. Wright, D. W. Schindel, D. A. Hutchins, P. W. Carpenter, and D. P. Jansen, ''Ultrasonic tomographic imaging of temperature and flow fields in gases using air-coupled capacitance transducers,'' J. Acoust. Soc. Am. **104**, 3446–3455 (1998).
[18] J. M. S. Prewitt, ''Algorithms in computerized tomography,'' in *Medical Imaging Techniques—A Comparison* (Plenum, New York, 1979), pp. 287–312.
[19] K. T. Ladas and A. J. Devaney, ''Application of an ART algorithm in an experimental study of ultrasonic diffraction tomography,'' Ultrason. Imaging **15**, 48–58 (1993).
[20] D. P. Jansen, D. A. Hutchins, P. J. Ungar, and R. P. Young, ''Acoustic tomography in solids using a bent ray SIRT algorithm,'' Nondestr. Test. Eval. **6**, 131–148 (1991).
[21] A. H. Delaney and Y. Bresler, ''A fast iterative tomographic reconstruction algorithm,'' Int. Conf. Acoust., Speech, & Signal Process. (1995), pp. 2295–2298.
[22] L. Wang and R. S. Granetz, ''Series expansion method in three-dimensional tomography,'' J. Opt. Soc. Am. A Opt. Image Sci. Vis. **10**, 2292–2295 (1993).
[23] H. H. Stark, J. W. Woods, I. Paul, and R. Hingorani, ''Direct Fourier reconstruction in computer tomography,'' IEEE Trans. Acoust., Speech, Signal Process. **29**, 237–245 (1981).
[24] A. J. Devaney, ''A fast filtered backpropagation algorithm for ultrasound tomography,'' IEEE Trans. Ultrason. Ferroelectr. Freq. Control **34**, 330–340 (1987).
[25] A. C. Kak and M. Slaney, *Principles of Computerized Tomographic Imaging* (IEEE, New York, 1988).
[26] T. H. Gan, D. A. Hutchins, D. R. Billson, and F. C. Wong, ''Ultrasonic Tomographic Imaging of Encased Highly-Attenuating Solid Media,'' J. Quant. Non-Destr. Eval. **13**, 131–152 (2001).
[27] D. W. Schindel, D. A. Hutchins, L. Zou, and M. Sayer, ''The design and characterization of micromachined air-coupled capacitive transducers,'' IEEE Trans. Ultrason. Ferroelectr. Freq. Control **42**, 42–50 (1995).
[28] R. Hickling and S. P. Marin, ''The use of Ultrasonics for gauging and proximity sensing in air,'' J. Acoust. Soc. Am. **79**, 1151–1160 (1986).